Inorg. Chem. **2007**, *46*, 5518–5527

Nonconjugated Dendritic Iridium(III) Complexes with Tunable Pyridine-Based Ligands: Synthesis, Photophysical, Electrochemical, and Electroluminescent Properties

Xianghong Li,[†] Zhao Chen,[‡] Qiang Zhao,[†] Li Shen,[†] Fuyou Li,*[,†] Tao Yi,[†] Yong Cao,*[,‡] and Chunhui Huang*[,†]

Department of Chemistry and Laboratory of Advanced Materials, Fudan University, Shanghai 200433, People's Republic of China, and Institute of Polymer Optoelectronic Materials and Devices, South China University of Technology, Guangzhou 510640, People's Republic of China

Received October 25, 2006

A simple synthetic route was developed for nonconjugated dendritic iridium(III) complex based on tunable pyridine-based ligands. From an intermediate 2-bromopyridyl-4-methanol, three series of polybenzyloxy dendritic pyridine-based ligands with 2-phenyl, 2-benzothienyl, and 2,4-difluorophenyl subsitituents were easily synthesized via two-step reactions (Suzuki reaction and etherifying reaction). Using these pyridine derivatives as the C^N ligands, these dendritic iridium(III) complexes exhibiting tunable photoluminescence from blue to red were obtained. The photoluminescence quantum yields of these dendritic complexes in neat films increased with the increasing generation number of dendritic C^N ligands. Importantly, these iridium complexes were used as dopants for successfully fabricating polymer-based electrophosphorescent light-emitting diodes (PLEDs) with the highest external quantum efficiency of 12.8%.

Introduction

Phosphorescent heavy-metal complexes (especially iridium(III) complexes) have recently attracted much attention[1−12] since the pioneering work of the Thompson and Forrest groups on the electrophosphorescent organic light-emitting diode (OLED).[13] Due to their relatively short excited-state lifetime, high photoluminescence efficiency, and excellent color tuning,[2,14] cyclometalated iridium(III) complexes are still the best phosphorescent dyes for OLEDs up to now. Although the iridium(III) complexes in dilute solution at room temperature show strong luminescence, consistent with strong spin−orbit coupling of the iridium(III) center, the intermolecular interaction at high concentrations leads to dimer, excimer, or aggregate formation, which can quench phosphorescence emission in the solid state.[15−17] The

* To whom correspondence should be addressed. Fax: 86-21-55664621. Tel: 86-21-55664185. E-mail: fyli@fudan.edu.cn (F.Y.L.); chhuang@pku.edu.cn (C.H.H.).

[†] Fudan University.

[‡] South China University of Technology.

(1) Baldo, M. A.; Lamansky, S.; Burrows, P. E.; Thompson, M. E.; Förrest, S. R. *Appl. Phys. Lett.* **1999**, *75*, 4.
(2) Lamansky, S.; Djurovich, P.; Murphy, D.; Abdel-Razzaq, F.; Lee, H. E.; Adachi, C.; Burrows, P. E.; Forrest, S. R.; Thompson, M. E. *J. Am. Chem. Soc.* **2001**, *123*, 4304−4312.
(3) Zhu, W.; Mo, Y.; Yuan, M.; Yang, W.; Cao, Y. *Appl. Phys. Lett.* **2002**, *80*, 2045−2047.
(4) Gong, X.; Ostrowski, J. C.; Bazan, G. C.; Moses, D.; Heeger, A. J. *Appl. Phys. Lett.* **2002**, *81*, 3711−3713.
(5) Chan, S. C.; Chan, M. C. W.; Wang, Y.; Che, C. M.; Cheung, K. K.; Zhu, N. *Chem. Eur. J.* **2001**, *7*, 4180−4190.
(6) Lu, W.; Mi, B. X.; Chan, M. C. W.; Hui, Z.; Che, C. M.; Zhu, N.; Lee, S. T. *J. Am. Chem. Soc.* **2004**, *126*, 4958−4971.
(7) Gawryszewska, P.; Sokolnicki, J.; Dossing, A.; Riehl, J. P.; Muller, G.; Legendziewicz, J. *J. Phys. Chem. A* **2005**, *109*, 3858−3863.
(8) (a) Zhao, Q.; Liu, S. J.; Shi, M.; Wang, C. M.; Yu, M. X.; Li, L.; Li, F. Y.; Yi, T.; Huang, C. H. *Inorg. Chem.* **2006**, *45*, 6152−6160. (b) Huang, C. H.; Li, F. Y.; Huang, W. *Introduction to Organic Light-Emitting Materials and Devices (in Chinese)*; Fudan University: Shanghai, 2005.
(9) Lundin, N. J.; Blackman, A. G.; Gordon, K. C.; Officer, D. L. *Angew. Chem., Int. Ed.* **2006**, *45*, 2582−2584.
(10) Yeh, S. J.; Wu, M. F.; Chen, C. T.; Song, Y. H.; Chi, Y.; Ho, M. H.; Hsu, S. F.; Chen, C. H. *Adv. Mater.* **2005**, *17*, 285−289.
(11) Suzuki, M.; Tokito, S.; Sato, F.; Igarashi, T.; Kondo, K.; Koyama, T.; Yamaguchi, T. *Appl. Phys. Lett.* **2005**, *86*, 103507.
(12) Yang, X. H.; Müller, D. C.; Neher, D.; Meerholz, K. *Adv. Mater.* **2006**, *18*, 948−954.
(13) Baldo, M. A.; O'Brien, D. F.; You, Y.; Shoustikov, A.; Sibley, S.; Thompson, M. E.; Forrest, S. R. *Nature* **1998**, *395*, 151−154.
(14) Lamansky, S.; Djurovich, P.; Murphy, D.; Abdel-Razzaq, F.; Kwong, R.; Tsyba, I.; Bortz, M.; Mui, B.; Bau, R.; Thompson, M. E. *Inorg. Chem.* **2001**, *40*, 1704−1711.
(15) Pope, M.; Swenberg, C. E. *Electronic Processes in Organic Crystals*; Clarendon: Oxford, 1982.
(16) Namdas, E. B.; Ruseckas, A.; Samuel, I. D. W.; Lo, S.-C.; Burn, P. L. *J. Phys. Chem. B* **2004**, *108*, 1570−1577.

10.1021/ic062041n CCC: $37.00 © 2007 American Chemical Society
Published on Web 06/05/2007

development of efficient OLEDs, therefore, requires a way of controlling the intermolecular interaction. Usually, doping cyclometalated iridium complexes into a host has been enthusiastically investigated as the main strategy to achieve highly efficient electrophosphorescnce devices.[18−23]Another approach is to introduce dendrimers into the molecular structures, owing to the three-dimensional hyperbranched structure of the dendrimers.[24−28]

Dendrimers based on the cores of the bipyridine ruthenium complexes[29,30] and rare-earth complexes[31−34] have been studied by many groups. However, the studies on dendritic iridium complexes are mainly limited to Samuel's work based on conjugated dendrimers.[35−46] Through the introduction of conjugated dendrons into the pyridine-based C^N ligands with Suzuki coupling reactions,[45] Samuel et al. synthesized some conjugated dendritic iridium(III) complexes and found that these dendritic complexes were beneficial to fabricate the electroluminescence (EL) devices. However, the obvious red-shifts of their absorption and emission bands were observed in these conjugated iridium dendrimers, and the possibility of color tuning is limited and the realization of pure blue emission becomes difficult. Recently, Burn et al.[46] reported that the bathochromic problem was addressed to some degree in the dendrimer containing 2-ethylhexyloxy surface groups, biphenyl-based dendrons, and a *fac*-tri[2-(2,4-difluorophenyl)pyridyl]iridium(III) core. This inspired us to further synthesize appropriate nonconjugated dendritic iridium complexes for three-color luminescent materials. Herein, we reported a smart synthetic procedure of 2-aryl-substituted pyridines which could easily be modified by nonconjugated polyether dendrons. Using these dendritic pyridine derivatives as cyclometalated C^N ligands, the nonconjugated dendritic iridium complexes with polyether dendrons $Ir(C^N\text{-}Gn)_2(LX)$ (see Scheme 1) were synthesized and characterized by their photophysical, electrochemical, and electroluminescent properties. Importantly, tunable photoluminescence from blue to red was observed for these dendritic iridium complexes on the basis of the pyridine-based ligands with 2-phenyl, 2-benzothienyl, and 2,4-difluorophenyl subsitituents.

Results and Discussion

Synthesis. It is well known that the emission color of iridium(III) complexes depends on the chemical structure of ligand and that the blue, green, and red emissions were observed for the iridium(III) complexes associated with the C^N ligands 2,4-difluorophenylpyridine (dfp),[47,48] 2-phenylpyridine (ppy),[2] and 2-benzothienylpyridine (btp)[2] (see Scheme 1), respectively. Herein, three types of iridium(III) complexes based on 2-arylpyridines (2-aryl = 2-phenyl, 2-benzothienyl, and 2,4-difluorophenyl) were used as the cores of these dendrimers to tune the phosphorescent emission from blue to red. These dendritic C^N ligands dfp, ppy, and btp with polyarylether dendron via methyloxy group were denoted as dfp-G*n*, ppy-G*n*, and btp-G*n* ($n = 1$ and 2) (see Scheme 1), respectively.

All these dendritic C^N ligands were synthesized through a key intermediate of 2-bromo-4-hydroxymethylpyridine (**4**), which was prepared from 2-bromo-4-methylpyridine (**1**) in three steps with good overall yield of ∼65% (see Scheme 2). Because of the high reaction activity of hydroxymethyl and bromo groups, compound **4** could be used as an important intermediate. Through this intermediate **4**, three series of the dendritic C^N ligands dfp-G*n*, ppy-G*n*, and btp-G*n* were easily synthesized through introduction of noncon-

(17) Baldo, M. A.; Adachi, C.; Forrest, S. R. *Phys. Rev. B* **2000**, *62*, 10967−10977.
(18) Adachi, C.; Baldo, M. A.; Forrest, S. R.; Lamansky, S.; Thompson, M. E.; Kwong, R. C. *Appl. Phys. Lett.* **2001**, *78*, 1622−1624.
(19) Su, Y. J.; Huang, H. L.; Li, C. L.; Chien, C. H.; Tao, Y. T.; Chou, P. T.; Satta, S.; Liu, R. S. *Adv. Mater.* **2003**, *15*, 884−888.
(20) Tsuboyama, A.; Iwawaki, H.; Furugori, M.; Mukaide, T.; Kamatani, J.; Igawa, S.; Moriyama, T.; Miura, S.; Takiguchi, T.; Okada, S.; Hoshino, M.; Ueno, K. *J. Am. Chem. Soc.* **2003**, *125*, 12971−12979.
(21) Zhao, Q.; Jiang, C. Y.; Shi, M.; Li, F. Y.; Yi, T.; Cao, Y.; Huang, C. H. *Organmetalics* **2006**, *25*, 3631−3638.
(22) Jiang, J. X.; Xu, Y. H.; Yang, W.; Guan, R.; Liu, Z. Q.; Zhen, H. Y.; Cao, Y. *Adv. Mater.* **2006**, *18*, 1769−1773.
(23) Gong, X.; Robinson, M. R.; Ostrowski, J. C.; Moses, D.; Bazan, G. C.; Heeger, A. J. *Adv. Mater.* **2002**, *14*, 581−585.
(24) Newkome, G. R.; Moorefield, C. N.; Vögtle, F. *Dendrimers and dendrons: Concepts, Synthesis, Applications*; VCH: Weinheim, Germany, 2001.
(25) Fréchet, J. M. J.; Tomalia, D. A.; Eds. *Dendrimers and other Dendric polymers;* Wiley: Chichester, U.K., 2001.
(26) Grayson, S. M.; Fréchet, J. M. J. *Chem. Rev.* **2001**, *101*, 3819−3868.
(27) Ranasinghe, M. I.; Varnavski, O. P.; Pawlas, J.; Hauck, S. I.; Louie, J.; Hartwig, J. F.; Goodson, T. *J. Am. Chem. Soc.* **2002**, *124*, 6520−6521.
(28) Dichtel, W. R.; Hecht, S.; Fréchet, J. M. J. *Org. Lett.* **2005**, *7*, 4451−4454.
(29) Vögtle, F.; Plevoets, M.; Nieger, M.; Azzellini, G. C.; Credi, A.; Cola, L. D.; Marchis, V. D.; Venturi, M.; Balzani, V. *J. Am. Chem. Soc.* **1999**, *121*, 6290−6298.
(30) Glomm, W. R.; Volden, S.; Sjoblom, J.; Lindgren, M. *Chem. Mater.* **2005**, *17*, 5512−5520.
(31) Pollak, K. W.; Leon, J. W.; Fréchet, J. M. J.; Maskus, M.; Abruna, H. D. *Chem. Mater.* **1998**, *10*, 30−38.
(32) Kawa, M.; Takahagi, T. *Chem. Mater.* **2004**, *16*, 2282−2286.
(33) Li, S. F.; Zhong, G. Y.; Zhu, W. H.; Li, F. Y.; Pan, J. F.; Huang, W.; Tian, H. *J. Mater. Chem.* **2005**, *15*, 3221−3228.
(34) Shen, L.; Shi, M.; Li, F. Y.; Li, X. H.; Shi, E. X.; Yi, T.; Du, Y. K.; Huang, C. H. *Inorg. Chem.* **2006**, *45*, 6188−6197.
(35) Lupton, J. M.; Samuel, I. D. W.; Frampton, M. J.; Beavington, R.; Burn, P. L. *Adv. Funct. Mater.* **2001**, *11*, 287−294.
(36) Markham, J. P. J.; Lo, S.-C.; Magennis, S. W.; Burn, P. L.; Samuel, I. D. W. *Appl. Phys. Lett.* **2002**, *80*, 2645−2647.
(37) Anthopouls, T. D.; Markham, J. P. J.; Namdas, E. B.; Samuel, I. D. W.; Lo, S.-C.; Burn, P. L. *Appl. Phys. Lett.* **2003**, *82*, 4824−4826.
(38) Namdas, E. B.; Ruseckas, A.; Samuel, I. D. W.; Lo, S.-C.; Burn, P. L. *Appl. Phys. Lett.* **2005**, *86*, 091104.
(39) Markham, J. P. J.; Samuel, I. D. W.; Lo, S.-C.; Burn, P. L.; Weiter, M.; Bässler, H. *J. Appl. Phys.* **2004**, *95*, 438−445.
(40) Lo, S.-C.; Male, N. A. H.; Markham, J. P. J.; Magennis, S. W.; Burn, P. L.; Salata, O. V.; Samuel, I. D. W. *Adv. Mater.* **2002**, *14*, 975−979.
(41) Anthopouls, T. D.; Frampton, M. J.; Namdas, E. B.; Burn, P. L.; Samuel, I. D. W. *Adv. Mater.* **2004**, *16*, 557−560.
(42) Namdas, E. B.; Anthopoulos, T. D.; Samuel, I. D. W.; Frampton, M. J.; Lo, S. C.; Burn, P. L. *Appl. Phys. Lett.* **2005**, *86*, 161104.
(43) Lo, S.-C.; Anthopoulos, T. D.; Namdas, E. B.; Burn, P. L.; Samuel, I. D. W. *Adv. Mater.* **2005**, *17*, 1945−1948.
(44) Ding, J. Q.; Gao, J.; Cheng, Y. X.; Xie, Z. Y.; Wang, L. X.; Ma, D. G.; Jing, X. B.; Wang, F. S. *Adv. Funct. Mater.* **2006**, *16*, 575−581.
(45) Lo, S.-C.; Namdas, E. B.; Burn, P, L.; Samuel, I. D. W. *Macromolecules* **2003**, *36*, 9721−9730.
(46) Lo, S.-C.; Richards, G. J.; Markham, J. P. J.; Namdas, E. B.; Sharma, S.; Burn, P. L. *Adv. Funct. Mater.* **2005**, *15*, 1451−1458.
(47) Adachi, C.; Kwong, C.; Djurovich, P.; Adamovich, V.; Baldo, M. A.; Thompson, M. E.; Forrest, S. R. *Appl. Phys. Lett.* **2001**, *79*, 2082−2084.
(48) You, Y. M.; Park, S. Y. *J. Am. Chem. Soc.* **2005**, *127*, 12438−12439.

Scheme 1. Chemical Structures of the Dendritic Iridium Complexes Ir(C^N-G*n*)$_2$(LX)

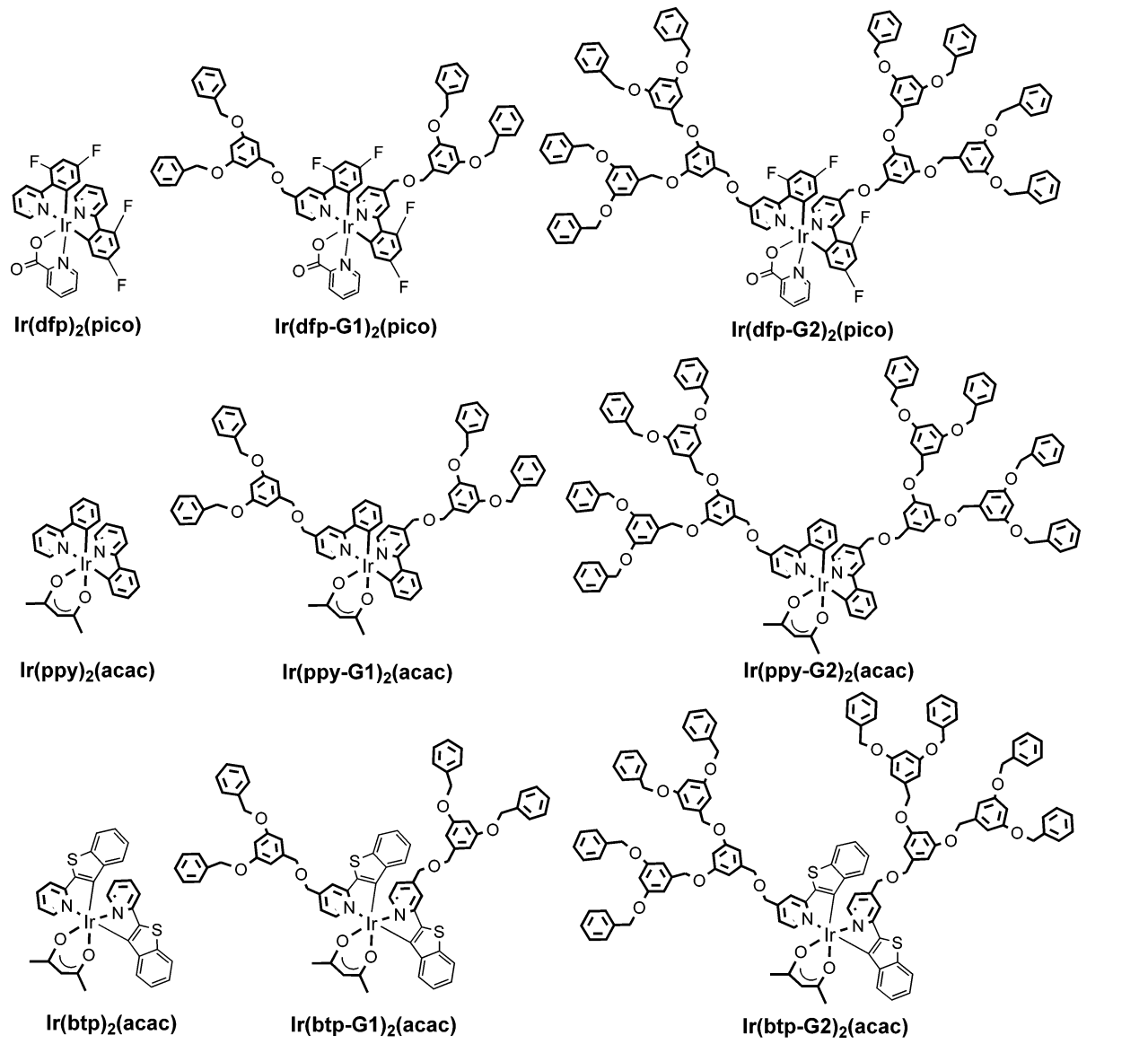

Scheme 2. Synthetic Route of 2-Bromopyridyl-4-methanol

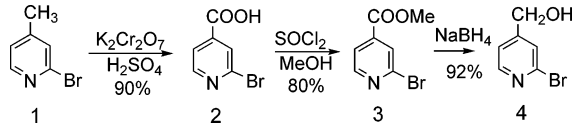

Scheme 3. Two Synthetic Strategies of ppy-G1

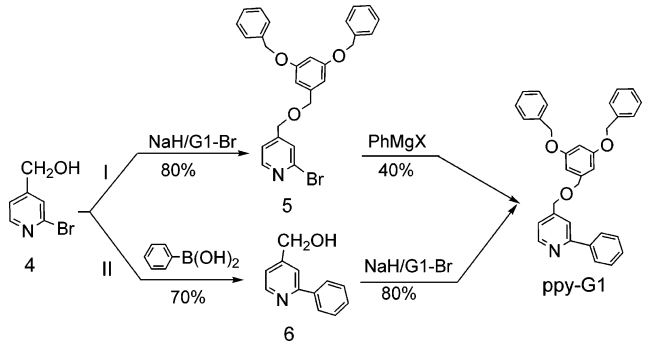

jugated polyarylether dendrons and different aryl groups. Two strategies were used to obtain the nonconjugated dendritic C^N ligands dfp-G*n*, ppy-G*n*, and btp-G*n*. Herein, the synthesis of ppy-G1 (as an example) is discussed in detail (see Scheme 3). One synthetic strategy (I) of ppy-G1 was to attach 3,5-(dibenzyl)benzyl bromide (G1-Br)[31,49] to the 4-hydroxymethyl group of **4** and then to replace the bromo group with a phenyl substituent using Kharash-coupling reaction. However, in this way, the ether bond was partly ruptured in Kharash reaction, resulting in a low yield (<40%) and the formation of a byproduct, 4-hydroxymethylpyridine, which may be attributed to the fact that the strong basic property of the Grignard reagent facilitated the disconnection of C−O−C bond. The other synthetic strategy (II) of ppy-G1 (see Scheme 3) was to attach the aryl group first to 4-hydroxymethylpyridine by Suzuki reaction and then to incorporate the dendron. Compared with the strategy (I), this method (II) exhibited a higher overall yield (>50%) with a relatively simple purification procedure. Similarly, the other dendritic C^N ligands ppy-G2, btp-G*n*, and dfp-G*n* ($n = 1$

(49) Hawker, C. J.; Fréchet, J. M. J. *J. Am. Chem. Soc.* **1990**, *112*, 7638−7647.

Table 1. Photophysical Properties of the Dendritic Iridium(III) Complexes

complex	λ_{abs} ($\epsilon \times 10^4$ mol^{-1} L cm^{-1})	$\lambda_{em(sol)}$[a] (nm)	$\lambda_{em(film)}$/nm	τ_{sol}[a]/ns	τ_{film}/ns	Φ_{sol}[a]	Φ_{film}[b](%)
Ir(dfp)$_2$(pico)	257 (4.6), 280 (4.4), 382 (3.5), 427 (3.1)	472, 494(sh)	504	911	29	0.30	−
Ir(dfp-G1)$_2$(pico)	259 (4.7), 280 (4.5), 381 (3.7), 427 (3.3)	476, 494(sh)	517	1020	275	0.38	38
Ir(dfp-G2)$_2$(pico)	260 (4.7), 279 (4.6), 381 (3.8), 427 (3.3)	476, 494(sh)	480, 504	1224	373	0.49	77
Ir(ppy)$_2$(acac)	259 (4.7), 344 (4.0), 412 (3.7), 460 (3.6), 495 (3.2)	519	538	1130	11	0.25	−
Ir(ppy-G1)$_2$(acac)	263 (4.7), 345 (4.1), 412 (3.8), 462 (3.6), 493 (3.3)	528	535, 580(sh)	1224	51	0.27	8
Ir(ppy-G2)$_2$(acac)	275 (4.8), 343 (4.1), 412 (3.8), 460 (3.6), 493 (3.3)	530	531	1306	134	0.32	16
Ir(btp)$_2$(acac)	285 (4.5), 340 (4.3), 356 (4.2), 488 (3.8)	615, 670	619, 666	2005	54	0.14	−
Ir(btp-G1)$_2$(acac)	282 (4.6), 342 (4.3), 358 (4.2), 487 (3.9)	619, 675	624, 680	2510	179	0.17	5
Ir(btp-G2)$_2$(acac)	282 (4.8), 342 (4.4), 358 (4.3), 485 (3.9)	619, 674	624, 676	2820	895	0.21	12

[a] Luminescence lifetime and quantum efficiency measurements were made in THF solution at 298 K. The lifetimes have error bars of ±10%, and the luminescence quantum efficiencies in solution have error bars of ±1% [b] The luminescence quantum efficiencies in neat films have error bars of ±20%.

Table 2. Electrophosphorescent Data for the PLED Devices from Ir(ppy-G*n*)$_2$(acac) and Ir(btp-G*n*)$_2$(acac) Doped into PFO−PBD as Host[a]

device	material	wt % (%)	L_{max} (cd/m^2)	*V* (V)	*LE* (cd/A)	*EQE* (%)	λ_{max} ^{EL} nm	CIE (*x*,*y*)
I	Ir(ppy$_2$(acac)	2	12712	5.8	9.5	9.5	526	(0.35,0.60)
II	Ir(ppy-G1)$_2$(acac)	2	10529	4.8	18.8	12.8	530	(0.39,0.57)
III	Ir(ppy-G1)$_2$(acac)	4	10048	5.1	18.0	12.4	531	(0.40,0.57)
IV	Ir(ppy-G2)$_2$(acac)	2	9928	6.3	12.9	9.5	532	(0.40,0.57)
V	Ir(ppy-G2)$_2$(acac)	4	18584	7.7	12.5	9.5	533	(0.41,0.56)
VI	Ir(btp)$_2$(acac)	2	2403	5.8	2.4	6.0	620	(0.66,0.33)
VII	Ir(btp-G1)$_2$(acac)	2	2478	5.8	3.3	6.0	621	(0.64,0.37)
VIII	Ir(btp-G1)$_2$(acac)	4	2304	5.8	3.8	6.0	621	(0.64,0.36)
IX	Ir(btp-G2)$_2$(acac)	2	1159	6.5	2.4	6.0	621	(0.64,0.33)
X	Ir(btp-G2)$_2$(acac)	4	1285	7.7	2.5	6.3	619	(0.65,0.33)

[a] L_{max}: maximum luminance; *V*: operating voltage at 1 cd m^{-2}; LE: luminance efficiency at 100 cd/m^2; EQE: external quantum efficiency.

Scheme 4. Synthetic Route of the Dendritic Iridium Complexes

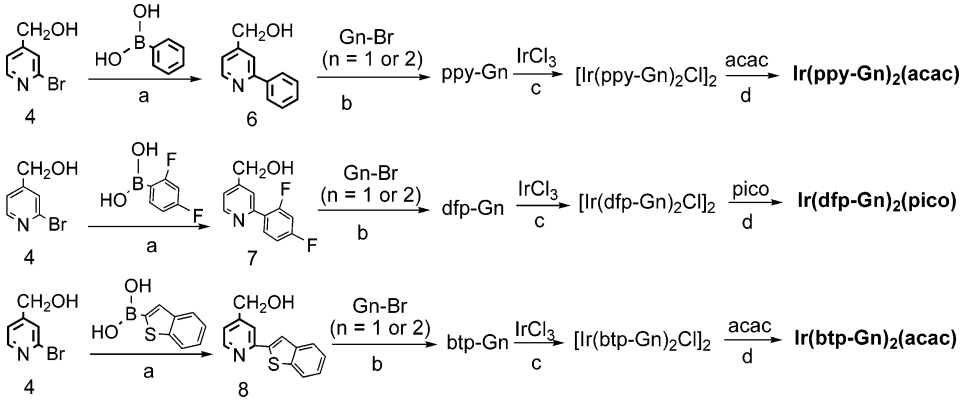

(a) $Pd(PPh_3)_4$, Na_2CO_3, PhMe, EtOH, H_2O, 100 °C; (b) NaH, THF, 3 h; (c) 2-ethoxyethanol, H_2O, 120 °C; (d) Na_2CO_3, 100 °C.

and 2) (see Scheme 1) were also obtained in moderate yields and characterized by NMR, Maldi-TOF mass spectra, and elemental analysis.

All the dendritic iridium(III) complexes (see Scheme 1) have two dendritic cyclometalated C^N ligands and an ancillary ligand, such as picolinic acid (pico) for Ir(dfp-G*n*)$_2$(pico) and acetylacetone (acac) for Ir(ppy-G*n*)$_2$(acac) and Ir(btp-G*n*)$_2$(acac). According to the previous literature reported by Nonoyama,[50] the synthetic method of these dendritic iridium complexes Ir(C^N-G*n*)$_2$(LX) involved two steps (see Scheme 4). The cyclometalated iridium(III) μ-chloro-bridged dimers (C^N)$_2$Ir(μ-Cl)$_2$Ir(C^N)$_2$ were synthesized by heating iridium chloride trihydrate ($IrCl_3 \cdot 3H_2O$) with an excess of the dendritic 2-arylpyridine derivatives (dfp-G*n*, ppy-G*n*, or btp-G*n*) in aqueous 2-ethoxyethanol, and then the iridium(III) complexes were prepared by the reaction of dimer with the corresponding ancillary monoanionic ligands (LX = acac or pico), in the presence of sodium carbonate. The overall yields of the dendrimers Ir(dfp-G*n*)$_2$(pico), Ir(ppy-G*n*)$_2$(acac), and Ir(btp-G*n*)$_2$(acac) were calculated to be 60−65%, 35−45%, and 45−60%, respectively.

All the complexes were successfully characterized through NMR, MALDI-TOF mass spectra, and elemental analysis. The ^{1}H NMR spectra of these complexes were more complicated than those of the small molecular iridium complexes Ir(dfp)$_2$(pico), Ir(ppy)$_2$(acac), and Ir(btp)$_2$(acac). The integral ratios of the protons of the surface phenyl groups to the aromatic region were in agreement with the stiochiometry of the dendritic complexes. The obvious proton signals of all methylene groups were observed. Moreover, thermal gravimetric analysis of these dendritic complexes was also carried out at a heating rate of 10 °C/min under nitrogen. In each case, no significant weight loss was observed below 280 °C, indicating that introduction of the nonconjugated dendrons to the core of 2-arylpyridine iridium-

(50) Nonoyama, K. *Bull. Chem. Soc. Jpn.* **1974**, *47*, 467.

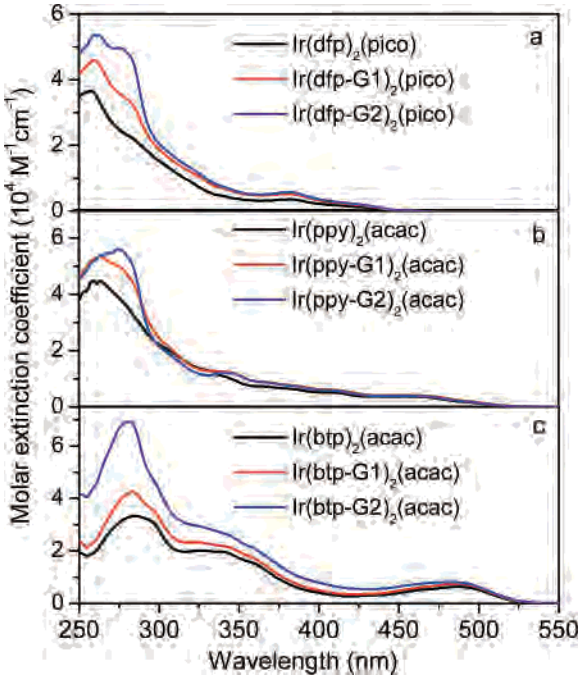

Figure 1. UV−vis absorption spectra of Ir(dfp-G*n*)$_2$(pico), Ir(ppy-G*n*)$_2$(acac), and Ir(btp-G*n*)$_2$(acac) in THF solutions ($c = 1.0 \times 10^{-5}$ mol L^{-1}).

(III) complex hardly influenced thermal stability of the dendritic complexes (see Supporting Information).

UV−vis Absorption Spectroscopy. The UV−vis absorption spectra of the dendritic complexes Ir(dfp-G*n*)$_2$(pico), Ir(ppy-G*n*)$_2$(acac), and Ir(btp-G*n*)$_2$(acac) ($n = 1$ and 2) in tetrahydrofuran (THF) solution are shown in Figure 1, and the data are listed in Table 1. All these complexes show intense absorption bands in the ultraviolet region at 250−350 nm with molar extinction coefficients (ϵ) of $\sim 10^4$ mol^{-1} L cm^{-1}, which are assigned to the spin-allowed $\pi \rightarrow \pi^*$ transitions of the C^N ligands and benzyloxy units. For these dendritic complexes, complexation of the dendritic C^N ligands to the iridium cation results in little difference in the absorption wavelengths of the ligands. However, the molar extinction coefficient at around 270 nm increased from the zero generation to the second generation, which is attributed to the increased number of benzyloxy units. For example, the ϵ values at 270 nm for Ir(ppy)$_2$(acac), Ir(ppy-G1)$_2$(acac), and Ir(ppy-G2)$_2$(acac) were 4.30×10^4, 5.15×10^4, and 5.60×10^4 mol^{-1} L cm^{-1} (see Figure 1), respectively. Somewhat weaker bands at lower energies were observed for Ir(dfp-G*n*)$_2$(pico), Ir(ppy-G*n*)$_2$(acac), and Ir(btp-G*n*)$_2$(acac). According to most of the previous reports about cyclometalated complexes,[51−54] these bands were assigned to singlet and triplet metal-to-ligand charge transfer (MLCT) transitions. For example, for Ir(ppy-G*n*)$_2$(acac), two MLCT bands are clearly resolved at 412 and 460 nm, with

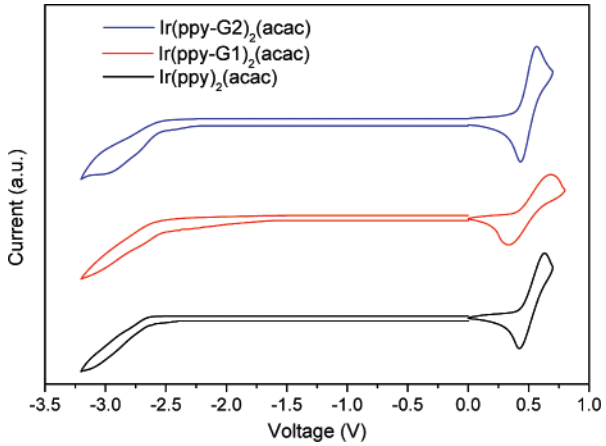

Figure 2. Cyclic voltammograms of Ir(ppy-G*n*)$_2$(acac) (scan rate = 50 mV s^{-1}).

extinction coefficients of ~4600 and 3800 M^{-1} cm^{-1}, respectively. In the cases of Ir(btp-G*n*)$_2$(acac), ^{1}MLCT and ^{3}MLCT were not clearly resolved, and a broad band was observed between 435 and 525 nm. Moreover, the spectra of the dendritic iridium complexes Ir(C^N-G*n*)$_2$(LX) are very similar to those of their corresponding small molecular iridium complexes Ir(C^N)$_2$(LX) with the same core of the C^N ligand, suggesting that the dominant absorptions in the dendritic iridium complexes Ir(C^N-G*n*)$_2$(LX) are due to the "Ir(C^N)$_2$" fragment.

Electrochemical Studies. Electrochemical properties of Ir(dfp-G*n*)$_2$(pico), Ir(ppy-G*n*)$_2$(acac), and Ir(btp-G*n*)$_2$(acac) ($n = 0-2$) in CH_2Cl_2 and THF solution were studied by the cyclic voltammetry, and the data are summarized in Table 2. As an example, Figure 2 shows the cyclic voltammograms of Ir(ppy-G*n*)$_2$(acac) with a scan rate of 50 mV s^{-1}. According to the equation $E_{HOMO(LUMO)} = -(4.80 + E_{onset})$,[55] the HOMO and LUMO energies of all complexes were calculated and the energy gap (E) between HOMO and LUMO can be deduced by the equation E = LUMO − HOMO. All complexes show reversible or quasireversible oxidation waves in the range of 0.46−1.18 V vs Ag/AgNO$_3$ by referencing ferrocene/ferrocenium as a standard. According to the previous electrochemical studies on iridium complexes, the oxidation waves are assigned to metal-centered Ir^{III}/Ir^{IV}oxidation process.[56] It can be seen from Table 2 that energy gaps are similar for the dendritic iridium-(III) complex with the same core. Therefore, introduction of dendritic framework changed scarcely the energy gaps of these series of iridium complexes.

Photoluminescent Properties. The room-temperature photoluminescence (PL) spectra of these iridium complexes in THF solution are shown in Figure 3, and the corresponding photophysical data are summarized in Table 1. It can be seen that all complexes emit intense luminescence at room temperature in THF solution. Three series of iridium complexes Ir(dfp-G*n*)$_2$(pico), Ir(ppy-G*n*)$_2$(acac), and Ir(btp-

(51) Colombo, M. G.; Brunold, T. C.; Riedener, T.; Güdel, H. U. *Inorg. Chem.* **1994**, *33*, 545−550.
(52) (a) Garces, F. O.; King, K. A.; Watts, R. J. *Inorg. Chem.* **1988**, *27*, 3464−3471. (b) Carlson, G. A.; Djurovich, P. I.; Watts, R. J. *Inorg. Chem.* **1993**, *32*, 4483−4484.
(53) Serroni, S.; Juris, A.; Campagna, S.; Venturi, M.; Denti, G.; Balzani, V. *J. Am. Chem. Soc.* **1994**, *116*, 9086−9091.
(54) Neve, F.; Deda, M. L.; Crispini, A.; Bellusci, A.; Puntoriero, F.; Campagna, S. *Organometallics* **2004**, *23*, 5856−5863.
(55) Thomas, K. R. J.; Velusamy, M.; Lin, J. T.; Chien, C. H.; Tao, Y. T.; Wen, Y. S.; Hu, Y. H.; Chou, P. T. *Inorg. Chem.* **2005**, *44*, 5677−5685.
(56) Wu, F. I.; Su, H. J.; Shu, C. F.; Luo, L. Y.; Diau, W. G.; Cheng, C. H.; Duan, J. P.; Lee, G. H. *J. Mater. Chem.* **2005**, *15*, 1035−1042.

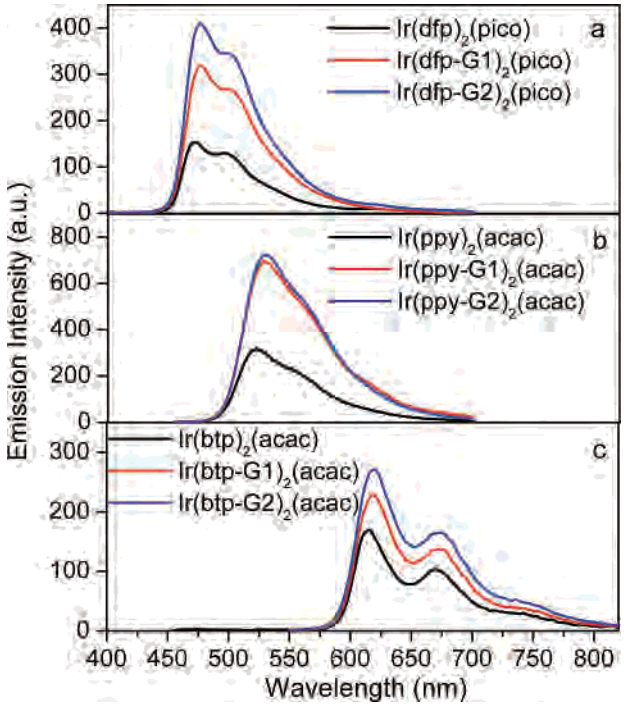

Figure 3. Room-temperature photoluminescence spectra of the dendritic complexes (5×10^{-6} M) in THF solution (λ_{ex}= 360 nm).

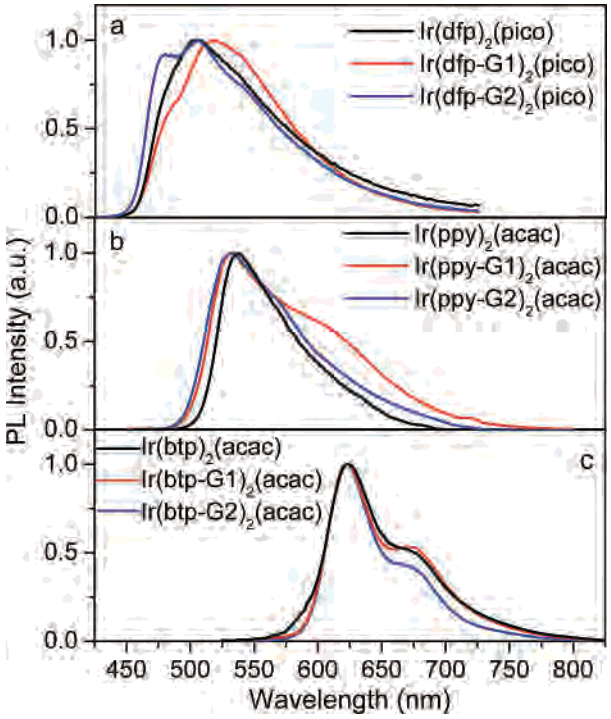

Figure 4. Photoluminescence spectra of the dendritic iridium complexes in neat films (λ_{ex} = 360 nm).

G*n*)$_2$(acac) in THF solution exhibit emission bands centered at ~476, 520, and 619 nm (see Table 1), respectively, indicating that they are blue, green, and red light-emitting materials. The luminescence lifetimes (τ) of these dendritic iridium complexes, measured at 298 K in degassed solution, are in the range of 0.92−2.75 μs (see Table 1). Such long-lived excited states and their sensitivity toward oxygen indicate that the emitting states of these iridium complexes have triplet character.[2] Moreover, the photoluminescence spectra of Ir(dfp-G*n*)$_2$(pico) and Ir(ppy-G*n*)$_2$(acac) are broad and featureless, indicating that the emission originates primarily from the ^{3}MLCT state. However, fine vibronic structures were observed in the emission spectra of Ir(btp-G*n*)$_2$(acac), corresponding to a significant ligand^3($\pi-\pi^*$) contribution to the phosphorescence.[57]

It can be seen from Table 1 that the introduction of polyarylether dendrons into the C^N ligands results in a minor perturbation on the emission properties of these iridium(III) complexes in solution. All of the dendritic complexes in solution with the same core of Ir(C^N)$_2$(LX) show similar emission bands (see Figure 3), and no obvious improvements on the photoluminescence quantum yields (ϕ) and lifetimes of the dendritic complexes were observed with increasing in the dendritic generation. For example, the photoluminescence quantum yields of Ir(btp)$_2$(acac), Ir(btp-G1)$_2$(acac), and Ir(btp-G2)$_2$(acac) were calculated as 0.14, 0.17, and 0.21, respectively, corresponding to their luminescence lifetimes of 1130, 1204, and 1306 ns, respectively.

(57) (a) Sandrini, D.; Maestri, M.; Ciano, M.; Balzani, V.; Deuschel-Cornioley, C.; von Zelewsky, A.; Jolliet, P. *Helv. Chim. Acta* **1988**, *71*, 1053. (b) Balton, C. B.; Murtaza, Z.; Shaver, R. J.; Rillema, D. P. *Inorg. Chem.* **1992**, *31*, 3230.

Compared with no significant influence on the emission properties in solution, the introduction of the polyarylether dendrons affects greatly the solid-state emission properties of the dendritic iridium(III) complexes. Figure 4 shows the photoluminescence spectra of all complexes in neat films. It can be seen from Figures 3 and 4 that these dendritic complexes from fluid solution to solid-state film show red-shifts of emission bands to different extent (see Table 1), in agreement with previous result of cyclometalated iridium(III) MLCT emitters.[2,16,45,46] Compared with the zero generation dendritic complexes, the first generation dendritic complexes in a neat film exhibit slightly more red-shifted emission color. An obvious shoulder band on the lower-energy side was observed for Ir(ppy-G1)$_2$(acac) (see Figure 4b) from fluid solution to solid-state film. Because of the relatively small structure of first generation dendrons, the steric bulk of the dendritic ligand was insufficient to prevent the interaction of the ppy ligands significantly. However, this bathochromic problem could be addressed to some degree through introduction of the second generation dendrons. The photoluminescence band of Ir(ppy-G2)$_2$(acac) in neat film overlaps nearly that of Ir(ppy)$_2$(acac), showing that attachment of the second generation dendron changes the emission color slightly. In addition, it can be seen from Table 1 that the introduction of the polyarylether dendrons into the C^N ligands significantly improved the photoluminescence quantum yields (φ) and luminescence lifetimes (τ) of the iridium complexes. For Ir(btp-G*n*)$_2$(acac), the photoluminescence quantum yield of Ir(btp)$_2$(acac) in neat film was too weak to be measured, while the corresponding quantum yields of Ir(btp-G1)$_2$(acac) and Ir(btp-G2)$_2$(acac) increased to 5% and 12%, respectively. Moreover, the luminescence lifetimes of Ir(btp-G1)$_2$(acac) and Ir(btp-G2)$_2$(acac) were

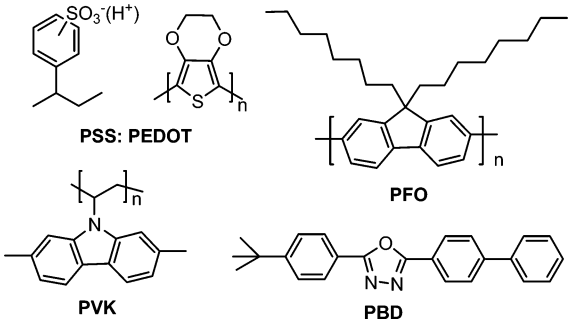

Figure 5. Chemical structures of accessorial materials used in PLEDs.

lengthened to 179 and 895 ns, respectively, in comparison with that of Ir(btp)$_2$(acac) (τ = 54 ns). These facts imply that the dendron's spread configuration weakens the intermolecular core−core interactions in solid state, and reduces the probability of phosphorescence quenching.[16,34]

Characterization of PLED Devices. Recently, polymer-based electrophosphorescent light-emitting diodes (PLEDs) have been paid a great deal of attention because they can be fabricated by solution processing and suitable for large-area and flexible display.[21−23,56,59−61] Herein, two series of dendritic iridium(III) complexes Ir(ppy-G*n*)$_2$(acac) and Ir(btp-G*n*)$_2$(acac) were used as emissive materials for PLEDs. The devices consist of a multilayer configuration ITO/PEDOT/PSS/PVK (40 nm)/PFO+PBD (30 wt %)/*x*% Ir-complex (80 nm)/Ba (4 nm)/Al (120 nm), where PVK is poly(vinylcarbazole) (see Figure 5). A thin film of PEDOT/PSS was spin-cast onto a precleaned ITO surface and then baked at 80 °C for 12 h under vacuum to improve hole injection and to increase substrate smoothness. Due to good hole-transporting properties, a layer of PVK was used as hole-transporting layer. Poly(9,9-dioctylfluorene) (PFO) was blended with 2-(4-biphenyl)-5-(4-tert-butylphenyl)-1,3,4-oxadiazole (PBD) because PBD is a good electron-transporting material.[62,63] The emitting layer, PFO−PBD (30 wt %) doped with 2% or 4% of these iridium complexes was then spin-cast onto the surface of PVK. Conjugated polymer PFO was chosen as the host material because of its high fluorescent quantum yield and good charge transporting property.

The electroluminescence data are summarized in Table 2. Compared the small molecular iridium complexes Ir(C^N)$_2$(LX) containing the same ancillary ligand with the corresponding dendritic complexes Ir(C^N-G*n*)$_2$(LX), no obvious variation was observed for the electroluminescence spectra, which means that introduction of the polyarylether dendrons into the C^N ligands did not alter the emissive wavelengths of the iridium complexes significantly. For example, in the case of Ir(btp-G*n*)$_2$(acac), the variation of dendron from zero generation to the second generation induced no obvious shifts (∼2 nm) of electrophorescence (see Table 2 and Supporting Information). The corresponding CIE chromaticity coordinates (*x*, *y*) were about (0.64, 0.36) for Ir(btp-G*n*)$_2$(acac), indicating that all EL devices with Ir(btp-G*n*)$_2$(acac) as dopant showed saturated red emission.

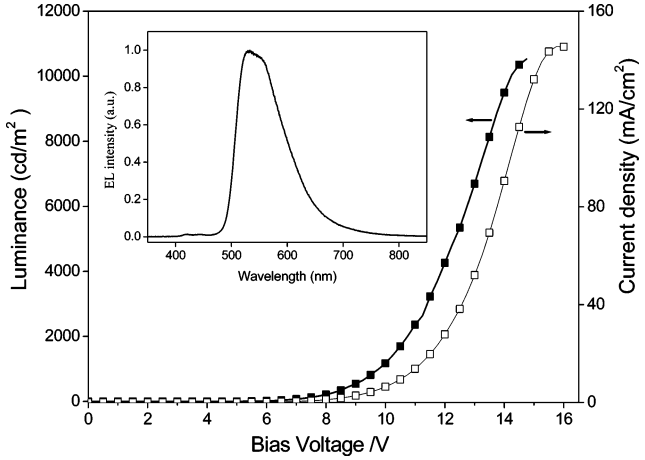

Figure 6. *I*−*V*−*L* characteristics for device *II* with the configuration of ITO/PEDOT/PSS/PVK (40 nm)/PFO+PBD (30 wt %)/2% Ir(ppy-G1)$_2$(acac) (80 nm)/Ba (4 nm)/Al (120 nm) Ir(ppy-G1)$_2$(acac). Inset: electroluminescent spectra of device *II*.

It can also be seen from Table 2 that all PLED devices with Ir(ppy-G*n*)$_2$(acac) as dopant exhibited excellent electrophosphorescence properties. As an example, Figure 6 shows the current density (*I*)−voltage (*V*)−luminance (*L*) characteristic of the device *II* [PVK (40 nm)/PFO+PBD (30 wt %)/2 wt % Ir(ppy-G1)$_2$(acac) (80 nm)/Ba(4 nm)/Al (120 nm)]. The PLED device *II* showed the maximum luminance of 10529 cd m^{-2} at 14.7 V, and the external quantum efficiency (EQE)[64] of 12.8% (see Table 2). For the device *IV* of Ir(ppy-G2)$_2$(acac) with a doping concentration of 2 wt %, the maximum luminescence was 9928 cd m^{-2}, and the external quantum efficiency was 9.5%. The corresponding CIE (Commission International de L'Eclairage) chromaticity coordinates (*x*, *y*) were (0.39, 0.57) and (0.41, 0.56) for Ir(ppy-G1)$_2$(acac) and Ir(ppy-G2)$_2$(acac), respectively, suggesting that all of Ir(ppy-G*n*)$_2$(acac) provided green emission. Moreover, when the doping concentration of Ir(ppy-G2)$_2$(acac) increased to 4 wt %, the maximum luminance of the PLED device *V* reached twice that of the 2 wt % doping concentration, and no obvious decrease in the luminous efficiency of device *V* was observed.

Conclusions

In summary, we have developed a simple synthetic route in incorporating dendrons into pyridine-based C^N ligands with different aryl groups via two-step reactions (Suzuki reaction and etherifying reaction) and successfully synthesized three series of nonconjugated dendritic iridium(III) complexes based on tunable pyridine-based ligands with 2-phenyl, 2-benzothienyl, and 2,4-difluorophenyl subsititu-

(58) Kawamura, Y.; Goushi, K.; Brooks, J.; Brown, J. J.; Sadabe, H.; Adachi, C. *Appl Phys. Lett.* **2005**, *86*, 071104.
(59) Chen, X. W.; Liao, J. L.; Liang, Y. M.; Ahmed, M. O.; Tseng, H. E.; Chen, S. A. *J. Am. Chem. Soc.* **2003**, *125*, 636−637.
(60) Gong, X.; Ostrowski, J. C.; Bazan, G. C.; Moses, D.; Heeger, A. J.; Liu, M. S.; Jen, A. K. Y. *Adv. Mater.* **2003**, *15*, 45−49.
(61) Jiang, C. Y.; Yang, W.; Peng, J. B.; Xiao, S.; Cao, Y. *Adv. Mater.* **2004**, *16*, 537−541.
(62) Adachi, C.; Tsutsui, T.; Saito, S. *Appl. Phys. Lett.* **1989**, *55*, 1489−1491.
(63) Kulkarni, A. P.; Tonzola, C. J.; Babel, A.; Jenekhe, S. A. *Chem. Mater.* **2004**, *16*, 4556−4573.
(64) Forrest, S. R.; Bradley, D. D.; Thompson, M. E. *Adv. Mater.* **2003**, *15*, 1043−1048.

ents. The emission of these dendritic complexes could be tuned from blue to red. Interestingly, the introduction of the nonconjugated dendrons did not significantly alter the emissive wavelengths of the core of the iridium complexes, but improved the solid-state luminescence quantum efficiencies of the iridium complexes. Moreover, by using these iridium complexes as dopants, PLEDs were successfully fabricated with the highest external quantum efficiency of 12.8%. Our synthetic route of nonconjugated dendritic ligands may open up broad prospects for designing other luminescent materials based on dendritic metal complexes.

Experimental Section

Materials. Poly(ethylendioxythiophene)/poly(styrene sulfonic acid) (PEDOT/PSS), conjugated poly(9,9-dioctylfluorene) (PFO), 2-(4-biphenyl)-5-(4-*tert*-butylphenyl)-1,3,4-oxadiazole (PBD), and 2-phenylpyridine (ppy) were purchased from Aldrich. Acetylacetone, 2-ethoxyethanol, 2-bromopyridine, 2-benzothienylboronic acid, 2,4-difluorophenylboronic acid, picolinic acid, and BuLi were obtained from Acros. $IrCl_3 \cdot 3H_2O$, $Pd(PPh_3)_4$, 2-bromo-4-methylpyridine, and 3,5-dihydroxybenzyl alcohol were industrial products and used without further purification. The Fréchet-type dendritic benzylic bromides [G-1]-Br and [G-2]-Br of first ($n = 1$) and second ($n = 2$) generation were prepared according to the general procedure developed by Hawer and Fréchet.[31,49] The small molecular C^N ligands 2-(2,4-difluorophenyl)pyridine (dfp) and 2-benzo[b]thiophenylpyridine (btp) were synthesized via the Suzuki-coupling reaction, using tetrakis(triphenylphosphine)palladium(0) and K_2CO_3 from 2-bromopyridine and corresponding boronic acid, according to previous references.[48,2]

General Experiments. NMR spectra were recorded on Varian Mercury Plus 400 MHz and Bruker AMX 500 MHz NMR spectrometers. UV−visible absorption spectra were recorded using a Shimadzu 2550 UV−vis−NIR spectrophotometer. The elemental analyses were performed on a VarioEL III O-Element Analyzer system. Mass spectra were obtained on a SHIMADZU matrix-assisted laser desorption/ionization time-of-flight mass spectrometer (MALDI-TOF-MASS). Thermal gravimetric analysis was performed on a Shimadzu thermogravimetric analyzer DTG-60H at a heating rate of 10 °C min^{-1} under nitrogen.

The photoluminescence spectra were measured on an Edinburgh LFS920 fluorescence spectrophotometer. Quantum efficiency measurements in THF solutions were carried out at room temperature. Before spectra were measured, the solutions were degassed by three freeze−pump−thaw cycles. The solution of quinine sulfate in 1 mol dm^{-3} sulfuric acid ($\Phi = 0.56$) was used as a reference.[65] The photoluminescent lifetime was recorded on a single photon counting spectrometer from Edinburgh Instrument (FLS920) with a hydrogen-filled pulse lamp as the excitation source. The data were analyzed by iterative convolution of the luminescence decay profile with the instrument response function using software package provided by Edinburgh Instruments.

Films were spin-coated from chloroform solutions with a dendrimer concentration of 10 mg mL^{-1} at 900 rpm for 1 min to give a thickness of about 150 nm. Their photoluminescence quantum yields in neat films were measured using an integrating sphere (UDT, Labsphere) and Omnichrome series 56 Helium Cadmium laser as the excitation source. The excitation wavelength was at 325 nm.

(65) Adams, M. J.; Highfield, J. G.; Kirkbright, G. F. *Anal. Chem.* **1977**, *49*, 1850−1852.

Electrochemical Measurements. Electrochemical measurements were carried out in a one-compartment cell under N_2 atmosphere, equipped with a glassy-carbon working electrode, a platinum wire counter electrode, and a Ag/Ag^+ reference electrode with an Eco chemie's Autolab. Measurements of oxidation and reduction were undertaken in the anhydrous solution of CH_2Cl_2 and THF, respectively, containing the supported electrolyte of a 0.10 mol L^{-1} tetrabutyl ammonium hexafluorophosphate ($Bu_4N^+ \cdot PF_6^-$). The scan rate was 100 or 50 mV s^{-1}.

Preparation of PLED Devices. An indium tin oxide (ITO) glass substrate with a sheet resistance of 15 Ω was kindly supplied by China Southern Glass Holding Co. Ltd. The fabrication of electrophosphorescent devices followed a standard procedure. A 70 nm thick layer of PEDOT/PSS was spin-cast onto precleaned ITO−glass substrates. A thin layer of Ba (4 nm thick) with a 200 nm thick Al capping layer was deposited through a shadow mask in a chamber with a base pressure of $\sim 10^{-4}$ Pa. Device fabrication was carried out in a controlled atmosphere drybox (Vacuum Atmosphere Co.) under N_2 circulation. Current density (I)−voltage (V)−luminance (L) data were collected using a Keithley 236 source measurement unit and a calibrated silicon photodiode. External electroluminescence (EL) quantum efficiencies were obtained by measuring the total light output in all directions in an integrating sphere (IS-080, Labsphere). The luminance (cd m^{-2}) and luminous efficiency (cd A^{-1}) were measured by a silicon photodiode and calibrated using a PR-705 SpectraScan spectrophotometer (Photo Research).

2-Bromo-4-methoxycarbonylpyridine (3).[66] A suspension of 7.4 g of 2-bromo-4-carboxypyridine (**2**) in 50 mL of thionyl chloride was refluxed for 4 h under inert atmosphere. The excess of thionyl chloride was distilled off, and the residue dried in a vacuum for 2 h. Absolute methanol (20 mL) was added, and the mixture refluxed for 1 h. Chloroform (100 mL) was then added, and the mixture was treated with a cold solution of sodium bicarbonate. The organic layer was dried on anhydrous sodium sulfate and the solvent removed in vacuum, 6.3 g of product was obtained without further purification, yield: 80%; ^{1}H NMR (δ, $CDCl_3$, 400 MHz): 8.53 (d, $J = 5.2$ Hz, 1H), 7.88 (d, $J = 8$ Hz,1H), 7.77 (dd, $J = 1.2$ Hz, $J = 4.8$ Hz, 1H), 3.96 (s, 3H).

4-Hydroxymethyl-2-bromopyridine (4). Sodium borohydride (1.7 g) was added in one portion to a suspension of the ester **3** (6.3 g) in 200 mL of ethanol. The mixture was refluxed for 3 h and cooled to room temperature, and then 200 mL of a saturated aqueous ammonium chloride solution was added to decompose the excess sodium borohydride. The ethanol was removed under vacuum, and the precipitated solid dissolved in a minimal amount of water. The resulting solution was extracted with ethyl acetate (5 × 200 mL) and dried over anhydrous sodium sulfate, and the solvent was removed under vacuum. The desired solid was obtained in 92% yield and was used without further purification. ^{1}H NMR (δ, $CDCl_3$, 400 MHz): 8.25 (d, $J = 5.2$ Hz, 1H), 7.35 (s, 1H), 7.20 (d, $J = 4.8$ Hz, 1H), 4.73 (s, 2H), 3.61 (s, 1H).

2-Phenylpyridyl-4-methanol (6). To a muxture of 5.1 g (27 mmol) of **4**, 3.65 g (30 mmol) of phenylboronic acid, and 0.155 g of $Pd(PPh_3)_4$ in deoxygenated toluene (150 mL), ethanol (15 mL) and an aqueous solution of potassium carbonate (2 M, 30 mL) were added. The resulting mixture was refluxed for 24 h. Cooling, filtration, extraction with chloroform, drying over anhydrous Na_2-

(66) Hamel, P.; Riendeau, D.; Brideau, C.; Chan, C.-C.; Desmarais, S.; Delorme, D.; Dube, D.; Ducharme, Y.; Ethier, D.; Grimm, E.; Falgueyret, J.-P.; Guay, J.; Jones, T. R.; Kwong, E.; AcAuliffe, M.; McFarlane, C. S.; Piechuta, H.; Roumi, M.; Tagari, P.; Young, R. N.; Girard, Y. *J. Med. Chem.* **1996**, *40*, 2866−2875.

SO_4, filtration, and solvent removal afforded to a crude product which was purified by chromatography on silica gel (light petroleum/chloroform, v/v = 3:1). A white powder (3.64 g) was obtained with a yield of 73%. ^{1}H NMR (δ, $CDCl_3$, 400 MHz): 8.63 (d, J = 5.2 Hz 1H), 7.98 (d, J = 6.8 Hz, 1H), 7.72 (s, 1H), 7.48−7.41 (m, 3H), 7.21 (d, J = 4.4 Hz 1H), 4.79 (s, 2H); *m*/*z* [EI]: 185.1 (M^+).

2-(2,4-Difluorophenyl)pyridyl-4-methanol (7). The similar procedure as described for 2-phenylpyridyl-4-methanol was used. ^{1}H NMR (δ, DMSO, 500 MHz): 8.64 (d, J = 5.0 Hz, 1H), 8.02−7.97 (m, 1H), 7.72 (s, 1H), 7.41−7.34 (m, 2H), 7.25−7.21 (m, 1H), 5.52 (t, J = 5.5 Hz, 1H), 4.62 (d, J = 6.0 Hz, 2H); ^{19}F NMR (δ, DMSO, 470 MHz): −108.62 to −108.69 (m, J_{HF} = 9.4 Hz, J_{HF} = 18.8 Hz, 1F), −111.81 to −111.87 (dd, J_{HF} = 9.4 Hz, J_{HF} = 18.8 Hz, 1F).

2-(Benzo[b]thiophen-2-yl)pyridyl-4-methanol (8). A similar procedure as that described for **6** was used. ^{1}H NMR (δ, $CDCl_3$, 400 MHz): 8.57 (d, J = 5.2 Hz, 1H), 7.87 (m, 2H), 7.79 (m, 2H), 7.36 (t, J = 4.4 Hz, 2H), 7.18 (d, J = 5.2 Hz, 2H), 4.80 (d, J = 5.6 Hz, 2H), 2.21 (t, J = 6.0 Hz, 1H); *m*/*z* [EI]: 241.1 (M^+); Anal. Calcd for $C_{14}H_{11}NOS$ (%): C 69.68, H 4.59, N 5.80, Found: C 69.82, H 4.68, N 5.69.

General Procedure for Synthesis of the Dendritic C^N Ligand. The dendritic C^N ligands dpf-G*n*, ppy-G*n*, and btp-G*n* (n = 1−2) were synthesized according to general procedure shown in Scheme 4. The corresponding 2-arylpyridyl-4-methanol (compound **6**, **7**, or **8**) (1.0 equiv) was dissolved in anhydrous tetrahydrofuran (THF), and NaH (excess) was added. [G*n*-Br] (n = 1−2) (2.5 equiv) was added after H_2 evolution ceased, and the reaction was stirred under argon for 4 h. Water was added slowly to quench any unreacted NaH, and the solution was extracted with CH_2Cl_2. The organic layer was dried over anhydrous K_2CO_3, and the solvent was removed under vacuum. The crude product was applied to a silica gel column and eluted with CH_2Cl_2, followed by 2−5% methanol in CH_2Cl_2. Yield: 50−70%.

dfp-G1. Yield: 65%: ^{1}H NMR (δ, DMSO, 500 MHz): 8.68 (d, J = 4.9 Hz, 1H), 8.03−7.98 (m, 1H), 7.73 (s, 1H), 7.43−7.30 (m, 12H), 7.24 (t, J = 7.8 Hz, 1H), 6.64 (s, 2H), 6.61 (s, 1H), 5.08 (s, 4H), 4.62 (s, 2H), 4.54 (s, 2H); ^{19}F NMR (δ, DMSO, 470 MHz): −108.40 to −108.47 (m, J_{HF} = 9.4 Hz, J_{HF} =18.8 Hz, 1F), −111.78 to −111.84 (dd, J_{HF} = 9.4 Hz, J_{HF} = 18.8 Hz, 1F). ^{13}C NMR (δ, $CDCl_3$, 125 MHz): 163.99, 163.89, 162.01, 161.91, 161.46, 161.37, 160.03, 159.47, 159.37,152.18, 150.18, 148.88, 140.90, 137.45, 132.76, 128.82, 128.22, 128.05, 124.16, 122.13, 122.06, 121.32, 112.57, 112.41, 106.84, 105.18, 104.97, 104.76, 101.60, 72.28, 70.18, 69.78; *m*/*z* [MALDI: CHCA]: 523.2 (M^+); Anal. Calcd for $C_{33}H_{27}F_2NO_3$ (%): C 75.70, H 5.20, N 2.68; Found: C 75.36, H 5.11, N 2.69.

dfp-G2. Yield: 70%: ^{1}H NMR (δ, DMSO, 500 MHz): 8.66 (d, J = 5.0 Hz, 1H), 8.02−7.99 (m, 1H), 7.73 (s,1H), 7.42−7.30 (m, 22H), 7.20 (m, 1H), 6.69 (s, 4H), 6.63− 6.60 (m, 5H), 5.06 (s, 8H), 5.01 (s, 4H), 4.62 (s, 2H), 4.54 (s, 2H), ^{19}F NMR (δ, DMSO, 470 MHz): −108.38 to −108.45 (m, J_{HF} = 9.4 Hz, J_{HF} = 18.8 Hz, 1F), −111.73 to −111.79 (dd, J_{HF} = 9.4 Hz, J_{HF} = 18.8 Hz, 1F). ^{13}C NMR (δ, DMSO, 100 MHz): 163.97, 163.87, 161.99, 161.89, 161.45, 161.35, 160.04, 159.93, 159.45, 159.35, 152.17, 150.19, 148.89, 140.89, 139.91, 137.38, 132.76, 132.71, 128.83, 128.26, 128.12, 124.14, 124.07, 122.14, 122.07, 121.31, 112.58, 112.41, 106.91, 105.19, 104.98, 104.77, 101.58, 72.27, 70.16, 69.80, 69.58; *m*/*z* [MALDI: CHCA]: 948.8 (M^+); Anal. Calcd for $C_{61}H_{51}F_2NO_7$(%): C 77.28, H 5.42, N 1.48; Found: C 76.66, H 5.72, N 1.13.

ppy-G1. Yield: 70%: ^{1}H NMR (δ, $CDCl_3$, 400 MHz): 8.66 (d, J = 4.8 Hz, 2H), 8.01 (d, J = 7.6 Hz, 2H), 7.72 (s, 2H), 7.49−7.32 (m, 13H), 7.20 (d, J = 4.8 Hz, 2H), 6.64 (s, 2H), 6.59 (s, 1H), 5.04 (s, 4H), 4.59 (s, 2H), 4.57 (s, 2H); ^{13}C NMR (δ, $CDCl_3$,-100 MHz): 160.45, 157.89, 150.02, 148.54, 140.45, 139.63, 137.09, 129.32, 129.06, 128.90, 128.32, 127.83, 120.70, 118.98, 106.96, 101.82, 72.94, 70.75, 70.36; *m*/*z* [MALDI: DI]: 487.7 (M^+), 595.5 ($M + Ag^+$); Anal. Calcd for $C_{33}H_{29}NO_3$ (%): C 81.29, H 5.99, N 2.87; Found: C 80.93, H 6.05, N 2.93.

ppy-G2. Yield: 73%: ^{1}H NMR (δ, $CDCl_3$, 400 MHz): 8.65 (d, J = 4.8 Hz, 1H), 8.00 (d, J = 7.6 Hz, 2H), 7.71 (s, 1H), 7.47−7.30 (m, 23H), 7.20 (d, J = 4.8 Hz, 1H), 6.67 (s,4H), 6.62 (s, 2H), 6.57 (s, 3H), 5.02 (s, 8H), 4.98 (s, 4H), 4.60 (s, 2H), 4.57 (s, 2H). ^{13}C NMR (δ, $CDCl_3$,100 MHz): 160.63, 160.53, 157.87, 150.16, 148.73, 140.74, 139.76, 139.69, 137.23, 129.50, 129.23, 129.03, 128.45, 128.02, 127.43, 120.83, 118.99, 107.13, 106.82, 101.96, 73.07, 70.89, 70.43, 70.33; *m*/*z* [MALDI: DI]: 911.9 (M^+), 1019.7 ($M + Ag^+$); Anal. Calcd for $C_{61}H_{53}NO_7$ (%): C 80.33, H 5.86, N 1.54; Found: C 79.60, H 5.94, N 1.55.

btp-G1. Yield: 75%: ^{1}HNMR (δ, $CDCl_3$, 400 MHz): 8.59 (d, J = 4.8 Hz, 1H), 7.85 (s, 2H), 7.79 (m, 2H), 7.42 (m, 12H), 7.15 (d, J = 4.8 Hz, 2H), 6.64 (s, 2H), 6.59 (s, 1H), 5.05 (s, 4H), 4.58 (s, 4H); ^{13}CNMR (δ, $CDCl_3$, 125 MHz): 160.21, 152.71, 149.70, 148.26, 144.74, 140.68, 140.45, 140.02, 136.80, 128.58, 128.00, 127.48, 124.48, 124.12, 122.55, 121.26, 117.65, 106.78, 101.67, 72.76, 70.24, 70.15; *m*/*z* [MALDI: DI]: 543.5 (M^+), 651.5 ($M + Ag^+$); Anal. Calcd for $C_{35}H_{29}NO_3S$ (%): C 77.32, H 5.38, N 2.58; Found: C 77.12, H 5.49, N 2.66.

btp-G2. Yield: 70%: ^{1}HNMR (δ, $CDCl_3$, 400 MHz): 8.59 (d, J = 4.8 Hz, 1H), 7.87−7.84 (m, 2H), 7.80 (s,1H), 7.78−7.76 (m, 2H), 7.42−7.30 (m, 22H), 7.17 (d, J = 4.8 Hz, 1H), 6.69 (d, 4H), 6.65 (d, 2H), 6.57 (s, 3H), 5.02 (s, 8H), 4.99 (s, 4H), 4.59 (d, 4H); ^{13}C NMR ($CDCl_3$, 100 MHz): 160.45, 160.35, 152.86, 149.91, 148.62, 144.90, 140.90, 140.71, 140.31, 139.49, 137.00, 128.87, 128.31, 127.85, 125.36, 124.80, 124.46, 122.84, 121.64, 121.10, 117.88, 107.02, 106.64, 101.86, 101.78, 73.04, 70.48, 70.35, 70.25; *m*/*z* [MALDI: DI]: 967.7 (M^+), 1075.5 ($M + Ag^+$); Anal. Calcd for $C_{63}H_{53}NO_7S$ (%): C 78.16, H 5.52, N 1.45; Found: C 77.29, H 5.43, N 1.50.

Cyclometalated Iridium Dendrimers Ir(dfp-G*n*)$_2$(pico), Ir(ppy-G*n*)$_2$(acac), and Ir(btp-G*n*)$_2$(acac) (n = 1,2). According to the Nonoyama's method,[50] cyclometalated Ir(III) μ-chloro-bridged dimers of a general formula $(C^N)_2Ir(\mu\text{-}Cl)_2Ir(C^N)_2$ were synthesized by refluxing $IrCl_3 \cdot nH_2O$ with 2.5 equiv of cyclometalating ligands dpf-G*n*, ppy-G*n*, or btp-G*n* in a mixture of 2-ethoxyethanol and water (3:1, v/v).

Ir(dfp)$_2$(pico), Ir(ppy)$_2$(acac), and Ir(btp)$_2$(acac) were prepared according to previous procedures.[2,10,14]

General Procedure for Synthesis of the Iridium Complexes Ir(dfp-G*n*)$_2$(pico). The corresponding chloro-bridged dimer complex (dfp-G*n*)$_2$Ir(μ-Cl)$_2$Ir(dfp-G*n*)$_2$ (0.08 mmol), 0.2 mmol of picolinic acid, and 85−90 mg of sodium carbonate were refluxed in an inert atmosphere in 2-ethoxyethanol for 10−12 h. After cooling to room temperature, a colored precipitate was filtered off and washed with water and ether. The crude product was flash chromatographed on a silica column with THF/hexane mobile phase, and the pure iridium complexes Ir(dfp-G*n*)$_2$(pico) were obtained with a yield of ∼60% after solvent evaporation and drying.

Ir(dfp-G1)$_2$(pico). Yellow solid, yield: 60%; ^{1}H NMR (δ, d^6-DMSO, 500 MHz): 8.50 (d, J = 6.0 Hz, 1H), 8.26 (s, 1H), 8.21 (s, 1H), 8.13 (m, 2H), 7.72 (m, 1H), 7.57 (m, 1H), 7.42 (m, 1H), 7.37−7.23 (m, 22H), 6.75−6.84 (m, 2H), 6.67−6.61 (m, 6H), 5.77 (d, J = 8.1 Hz, 1H), 5.55 (d, J = 8.1 Hz, 1H), 5.09 (s, 8H), 4.80

(d, 4H), 4.59 (d, J = 6.2 Hz, 4H); ^{19}F NMR (d^6-DMSO, 470 MHz): −106.66 to 106.68 (d, J_{HF} = 9.4 Hz, 1F), −107.44 to 107.46 (d, J_{HF} = 9.4 Hz, 1F), −108.83 (s, 1F), −109.37 (s, 1F); *m*/*z* [MALDI: DI]: 1466.5 (M + Ag$^+$); Anal. Calcd for $C_{72}H_{56}N_3O_8F_4$-Ir(%): C 63.61, H 4.15, N 3.09 Found: C 63.25, H 4.33, N 2.64; TGA (5%): 332.6 °C.

Ir(dfp-G2)$_2$(pico). Yellow solid, yield: 65%; ^{1}H NMR (δ, d^6-DMSO, 500 MHz): 8.48 (d, J = 6.0 Hz, 1H), 8.25 (s, 1H), 8.20 (s, 1H), 8.07 (m, 2H), 7.68 (m, 1H), 7.55−7.53 (m, 2H), 7.39−7.23 (m, 42H), 6.68∼6.60 (m, 20H), 5.75 (d, J = 8.0 Hz, 1H), 5.53 (d, J = 8.1 Hz, 1H), 5.05 (s, 16H), 5.00 (s, 8H), 4.81−4.78 (m, 4H), 4.59 (d, J = 7.0 Hz, 4H); ^{19}F NMR (d^6-DMSO, 470 MHz): −106.57 to 106.58 (d, J_{HF} = 9.4 Hz, 1F), −107.35 to 107.37 (d, J_{HF} = 9.4 Hz, 1F), −108.81 (s, 1F), −109.35 (s, 1F); *m*/*z* [MALDI: DI]: 2317.4 (M + Ag$^+$); Anal. Calcd for $C_{128}H_{104}N_3O_{16}F_4$-Ir(%): C 69.61, H 4.75, N 1.90; Found: C 68.85, H 4.79, N 1.44; TGA (5%): 337.5 °C.

General Procedure for Synthesis of the Iridium Complexes Ir(C^N)$_2$(acac). The corresponding chloro-bridged dimer complex (0.08 mmol), 0.2 mmol of acetyl acetone, and 85−90 mg of sodium carbonate were refluxed in an inert atmosphere in 2-ethoxyethanol for 10−12 h. After cooling to room temperature, a colored precipitate was filtered off and washed with water, hexane, and ether. The crude product was flash chromatographed on a silica column with a dichloromethane mobile phase, and the pure iridium complexes Ir(C^N)$_2$(acac) were obtained with a yield of 40−70% after solvent evaporation and drying.

Ir(ppy-G1)$_2$(acac). Yellow solid, yield: 45%: ^{1}H NMR (δ, $CDCl_3$, 400 MHz): 8.45 (d, J = 5.6 Hz, 2H), 7.80 (s, 2H), 7.55 (d, J = 7.6 Hz, 2H), 7.43−7.29 (m, 20H), 7.09 (d, J = 6.0 Hz, 2H), 6.79 (t, J = 7.6 Hz, 2H), 6.68 (m, 6H), 6.60 (s, 2H), 6.28 (d, J = 7.2 Hz, 2H), 5.20 (s, 1H), 5.07 (s, 8H), 4.71(s, 4H), 4.64 (s, 4H), 1.77 (s, 6H); *m*/*z* [MALDI: DI]: 1264.5 (M$^+$), 1372.2 (M + Ag$^+$); Anal. Calcd for $C_{71}H_{63}N_2O_8Ir$ (%): C 67.44, H 5.02, N 2.22, Found: C 67.00, H 4.99, N 2.26; TGA (5%): 306.6 °C.

Ir(ppy-G2)$_2$(acac). Yellow solid, yield: 40%: ^{1}H NMR (δ, $CDCl_3$, 400 MHz): 8.45 (d, J = 6.0 Hz, 2H), 7.78 (s, 2H), 7.52 (d, J = 7.6 Hz, 2H), 7.41−7.29 (m, 40H), 7.10 (d, J = 6.0 Hz, 2H), 6.75 (t, J = 7.2 Hz, 2H), 6.67 (m, 14H), 6.58 (m, 6H), 6.28 (d, J = 7.6 Hz, 2H), 5.17 (s, 1H), 5.01 (s,16H), 5.00 (s, 8H), 4.72 (s, 4H), 4.64 (s, 4H), 1.73 (s, 6H); *m*/*z* [MALDI: DI]: 2113.7 (M$^+$), 2221.7 (M + Ag$^+$); Anal. Calcd for $C_{127}H_{111}N_2O_{16}Ir$ (%): C 72.17, N 1.33, H 5.29; Found: C 72.16, N 1.05, H 5.16; TGA (5%): 324.2 °C.

Ir(btp-G1)$_2$(acac). Brown-red solid, yield: 60%. ^{1}H NMR (δ, $CDCl_3$, 400 MHz): 8.38 (d, J = 6.0 Hz, 2H), 7.60 (s, 3H), 7.58 (s, 1H), 7.44−7.30 (m, 20H), 7.04 (t, J = 8.0 Hz, 2H), 6.99 (d, J = 6.0 Hz, 2H), 6.82 (t, J = 7.6 Hz, 2H), 6.71 (d, J = 2.4 Hz, 4H), 6.63 (t, J = 2.4 Hz, 2H), 6.26 (d, J = 8.4 Hz, 2H), 5.25 (s, 1H), 5.09 (s, 8H), 4.78 (s, 4H), 4.68 (s, 4H), 1.77 (s, 6H); *m*/*z* [MALDI: DI]: 1376.1 (M$^+$), 1484.2 (M + Ag$^+$); Anal. Calcd for $C_{75}H_{63}N_2O_8IrS_2$ (%): C 65.43, N 2.03, H 4.61; Found: C 65.34, N 2.11, H 4.63; TGA (5%): 289.5 °C.

Ir(btp-G2)$_2$(acac). Brown-red solid, yield: 60%. ^{1}H NMR (δ, $CDCl_3$, 400 MHz): 8.38 (d, J = 6.0 Hz, 2H), 7.61 (s, 2H), 7.56 (d, J = 8.0 Hz, 2H), 7.40−7.29 (m, 40H), 6.99−6.95 (m, 4H), 6.78−6.68 (m, 14H), 6.60 (s,2H), 6.57 (s, 4H), 6.26 (d, J = 8.0 Hz, 2H), 5.22 (s, 1H), 5.02 (s, 8H), 5.00 (s, 16H), 4.80 (s, 4H), 4.68 (s, 4H), 1.74 (s, 6H); *m*/*z* [MALDI: DI]: 2226.7 (M$^+$), 2334.7 (M + Ag$^+$); Anal. Calcd for $C_{131}H_{111}N_2O_{16}IrS_2$ (%): C 70.69, N 1.26, H 5.03; Found: C 70.84, N 1.29, H 5.08; TGA (5%): 315.5 °C.

Acknowledgment. The authors are thankful for financial support from National Science Foundation of China (20490210 and 20501006), National High Technology Program of China (2006AA03Z318), Shanghai Sci. Tech. Comm. (05DJ14004 and 06QH14002) and Huo Yingdong Education Foundation (104012).

Supporting Information Available: *I*−*V*−*L* characteristics and electroluminescent spectra for the PLED device with the configuration of ITO/PEDOT/PSS/PVK (40 nm)/PFO+PBD (30 wt %)/*x*% Ir-complex (80 nm)/Ba (4 nm)/Al (120 nm) based on the phosphorescent emitters Ir(ppy-G*n*)$_2$(acac) and Ir(btp-G*n*)$_2$(acac). This material is available free of charge via the Internet at http://pubs.acs.org.

IC062041N